ACS Macro Letters

pubs.acs.org/macroletters Letter

Morphology and Dynamics of Coexisting Phases in Coacervate Solely Controlled by Crowded Environment

Qingwen Bai,‡ Xu Chen,‡ Jiaxin Chen, Zhijun Liu, Ya-nan Lin, Shuang Yang,* and Dehai Liang*

Cite This: ACS Macro Lett. 2022, 11, 1107−1111 Read Online

ACCESS | Metrics & More | Article Recommendations | Supporting Information

ABSTRACT: The membraneless organelles (MLOs) play a key role in the cell, yet it is unclear what controls the morphology and dynamics of MLOs in crowded cell medium. Using a biphasic coacervate droplet as a model of MLO, we online monitored the liquid−liquid phase separation process in crowded medium provided by poly(ethylene oxide) (PEO) or dextran. In PEO solution, which has an affinity with the inner phase, the spherical droplets evolve into clusters, networks, and completely phase inverted spheres in sequence with increasing PEO concentration, while in dextran solution, which has an affinity with the outer phase, the coacervates maintain the morphology but vary in phase ratio. Flower-like and even Janus structures are formed in the mixed PEO/dextran medium. Our work demonstrates that MLOs could be controlled solely by the crowded cell medium.

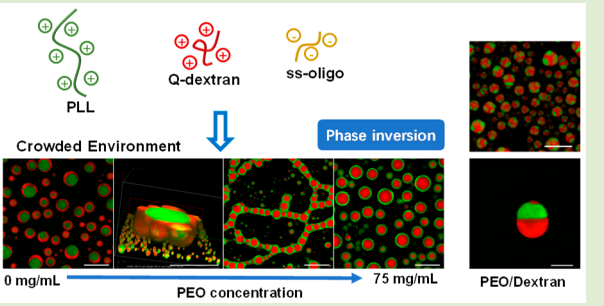

Membraneless organelles (MLOs), which are formed through intracellular coacervation or liquid−liquid phase separation (LLPS),[1] participate in many key cellular activities.[2−5] Some MLOs are proven to be hierarchical in structure, with immiscible subcompartments fulfilling different biofunctions.[6−8] Several biphase or multiphase coacervates[9−12] have been developed to unveil the basic principles behind these hierarchical structures. It is shown that the difference in interfacial energy and density of phases governs the formation and morphology of these coacervates.[13,14]

The MLOs are formed not in diluted solution, but in extremely crowded cytoplasm with the total macromolecular concentration up to 400 mg/mL.[15,16] It is well established that the macromolecular crowding and confinement from volume exclusion promotes the reactions or processes, resulting in decreased volume (e.g., protein folding),[17−21] and increases the effective reactant concentration.[22,23] Moreover, the non-specific interactions between the environment and targeted molecules also alter the molecular conformations.[24−27] It has been demonstrated that the crowded environment affects LLPS[28−30] by promoting droplet fusion,[31,32] generating denser coacervates,[33] and participating in the condensed phase.[28,34,35]

The presence of crowder in the solvent or its participation in phase separation inevitably varies the interfacial energy of the droplet.[36] In the case of multiphase coacervate, the change in the interfacial energy could tune the morphology, generating attractive hierarchical structures. To testify this hypothesis, we studied the coacervation of poly(L-lysine) (PLL), quaternized dextran (Q-dextran), and single-stranded oligonucleotide (ss-oligo) in crowded media provided by poly(ethylene oxide) (PEO) or dextran.

PLL/Q-dextran and ss-oligo solutions with equal amount of crowder were prepared separately beforehand. The biphasic coacervates were formed by mixing the two solutions with equal volume. The final concentrations of Q-dextran, PLL, and ss-oligo are 0.9, 0.5, and 1.5 mg/mL, respectively. Without crowder, PLL, Q-dextran, and ss-oligo spontaneously form biphasic coacervate droplets with PLL/ss-oligo being the internal phase and Q-dextran/ss-oligo being the external phase. As the positive charges and negative charges are balanced (± = 1.0), only one spherical phase is formed inside the droplet (Figure 1A,G). In PEO solution at 6.0 mg/mL, the PLL/ss-oligo droplets and Q-dextran/ss-oligo droplets connect with each other to form clusters (Figure S1). Eventually, the clusters transform into a giant PLL/ss-oligo core attached by several Q-dextran/ss-oligo droplets (Figure 1B). In 35.0 mg/mL PEO solution, the clusters are stable. The strand is composed of continuous PLL/ss-oligo phase with Q-dextran/ss-oligo droplets distributed inside (Figure 1C). The clusters turn into a coacervate network with increasing PEO concentration to 50.0 mg/mL, and the Q-dextran/ss-oligo droplets in the strand align into necklace structures (Figure 1D). In PEO solution at 75.0 mg/mL, spherical biphasic droplets similar to that in Figure 1A but with the phases completely inversed are formed (Figure 1E,H). The droplet size decreases with further

Received: July 14, 2022
Accepted: August 24, 2022
Published: August 25, 2022

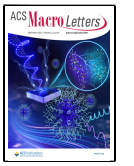

https://doi.org/10.1021/acsmacrolett.2c00409
ACS Macro Lett. 2022, 11, 1107−1111

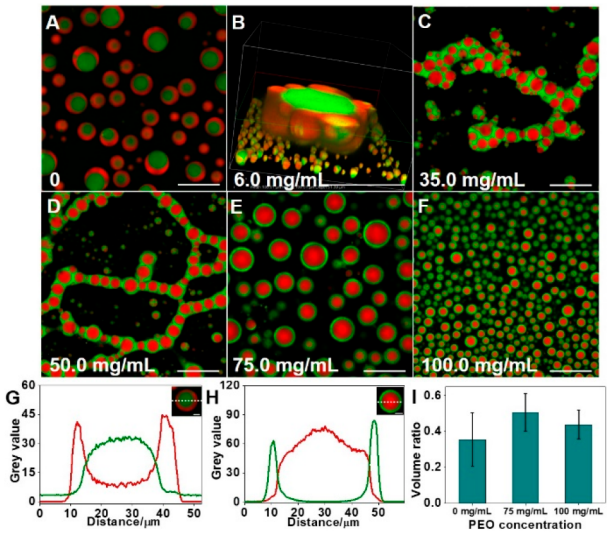

Figure 1. Coacervates of Q-dextran/PLL/ss-oligo incubated for 2 h in PEO solution at concentrations of (A) 0, (B) 6.0, (C) 35.0, (D) 50.0, (E) 75.0, and (F) 100.0 mg/mL. The concentrations of Q-dextran, PLL, and ss-oligo are 0.9, 0.5, and 1.5 mg/mL, respectively. The Q-dextran/ss-oligo phase is marked by red, and the PLL/ss-oligo phase by green. Scale bar: 50 μm. (G) and (H) compare the line profiles of fluorescence intensity across biphasic droplets in (A) and (E), respectively. (I) shows the volume ratio of the internal phase vs the whole droplet.

increasing PEO concentration (Figure 1F), which can be attributed to the macromolecular confinement effect.[37] The internal PLL/ss-oligo phase occupies 35% of the droplet volume in the control group (Figure 1I), while it occupies 51% and 47% of the total droplet volume in 75.0 mg/mL PEO and 100.0 mg/mL PEO, respectively. The content ratios demonstrate that the PLL/ss-oligo phase is more compatible with PEO solution.

The PLL/Q-dextran/ss-oligo coacervates were formed through growth, fusion, and maturation (Figure S1). Without PEO, the biphasic droplets grow larger via Brownian motion coalescence, in which the exterior Q-dextran/ss-oligo phase fuse with each other, followed by the fusion and relaxation of interior PLL/ss-oligo phase into spherical shape.[38] In PEO solution at 6.0 mg/mL, similar process is observed. However, the PLL/ss-oligo subcompartments inside the droplet cannot fuse into one phase in due course, forming biphasic coacervate droplet with worm-like structure (Figure 2A and Movie S1). In 50.0 mg/mL PEO solution, the fusion of PLL/ss-oligo phases into spherical shape is more severely hindered. Both Q-dextran/ss-oligo phase and PLL/ss-oligo phase serve as the connection points, arranging the droplets into a branched and then network structure (Figure 2B and Movie S2). In 75.0 mg/mL PEO solution, the fusion of PLL/ss-oligo phase becomes the leading process, while the Q-dextran/ss-oligo phase is internalized with time (Figure 2C and Movie S3). Eventually, the cluster evolves into a spherical biphasic droplet after about 2 h (inset in last panel of Figure 2C).

Coarse-grained modeling is applied to simulate the phase inversion process induced by PEO. Since the unit for LLPS is the primary complex at +/− = 1.0,[37] and the electrostatic attraction between oppositely charged polymers can be casted into an immiscibility between the polymer and solvent,[39] the primary complexes of Q-dextran/ss-oligo and PLL/ss-oligo are treated as neutral polymers **A** and **B**, respectively. Only short-

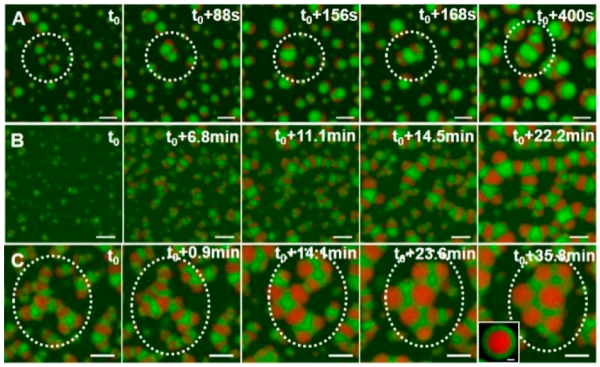

Figure 2. Coacervation processes of PLL/Q-dextran/ss-oligo in PEO solution at (A) 6.0, (B) 50.0, and (C) 75.0 mg/mL. The inset in last panel shows the matured state after 2 h. The t_0 for (A), (B), and (C) are 4.9, 6.1, and 21.5 min, respectively. Scale bar: 5 μm.

range interactions are considered. The hydrophobicity of these polymers follows **B** > **A** ≫ **PEO**. **PEO** is set to has affinity with **B**, as shown by its sequestration into PLL/oligo phase (Figure S3) and as reported in literature.[40] Details of simulation are listed in the Supporting Information. Results show that coacervate droplets are formed in all the studied n_{PEO}/n_B range, and the system exhibits a dilute phase and two condensed phases of polymers **A** and **B** (Figure 3). Without

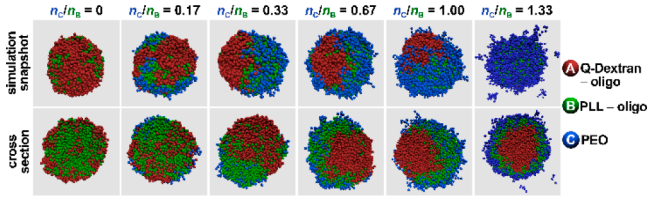

Figure 3. Snapshots of the coacervation droplets with increasing PEO content as obtained from coarse-grained simulations. Red, green, and blue particles denote polymers **A**, **B**, and **PEO**, respectively. The solvent molecules are not shown. The second row displays the snapshots of the cross-section at midpoint of the coacervate droplets.

PEO (n_{PEO}/n_B = 0), the **B** polymers are wrapped by its **A** counterparts. The phase separation within droplet originates from the hydrophobicity difference of **A** and **B**, and the more hydrophobic **B** polymers take up the inner space to avoid the disadvantageous **B**−solvent interface, which agrees with the experimental results.[39,40] Hydrophilic **PEO** can penetrate into the **B** phase due to their affinity, decreasing the hydrophobicity of phase **B** and thus making the contacts of solvents with **B**−**C** phase more favorable than that with the phase **A**. At n_{PEO}/n_B = 0.17 and 0.33, a small amount of **PEO** begin to bind with **B**, reducing the immiscibility between phase **B** and solvent. Meanwhile, the droplets turn to Janus shape to lower interfacial free energy of the system. At n_{PEO}/n_B = 0.67 and 1.00, **A** phase is barely wrapped by the less hydrophobic **B**/**PEO** mixture. Complete phase inversion occurs at n_{PEO}/n_B = 1.33. The radial density profiles of each species (Figure S2) clearly demonstrate that the droplets adopt well-defined core−shell structure at n_C/n_B = 0 and 1.33, but with **A** and **B** phases completely inverted.

As a crowder, dextran exhibits an effect different from that of PEO. The droplets maintain their original shape and structure in dextran solutions up to 150.0 mg/mL (Figure 4A−E). Dextran shares the same backbone with Q-dextran and is

https://doi.org/10.1021/acsmacrolett.2c00409
ACS Macro Lett. 2022, 11, 1107−1111

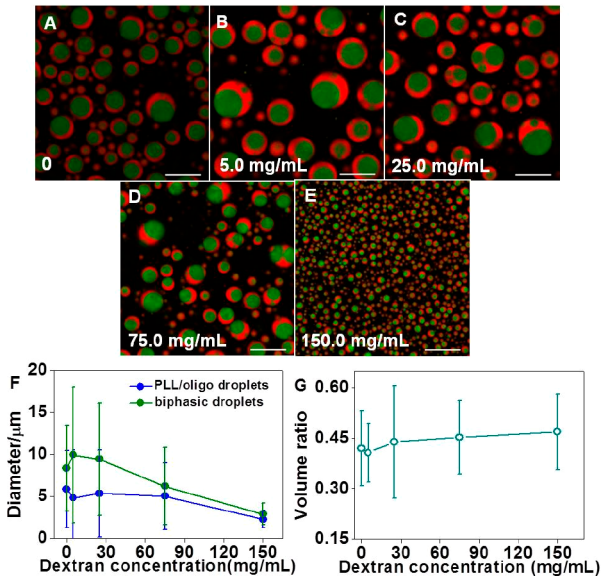

Figure 4. Coacervate droplets of Q-dextran/PLL/ss-oligo at 50 min in dextran solution at concentrations of (A) 0, (B) 5.0, (C) 25.0, (D) 75.0, and (E) 150.0 mg/mL. Scale bar: 25 μm. (F) and (G) show, respectively, the average diameters of the internal phase and the whole droplet, as well as their ratio, at different dextran concentrations. The vertical lines represent the size or volume ratio distribution of the coacervates.

compatible with the Q-dextran/ss-oligo phase.[38] Therefore, small amount of dextran (<25.0 mg/mL) in the environment facilitates the formation of Q-dextran/ss-oligo phase but hinders the PLL/ss-oligo phase, resulting in a droplet with smaller internal phase (Figure 4F,G). With furthering increasing dextran concentration to 150.0 mg/mL, the neutral dextran participated in the continuous phase weakens the electrostatic interaction between Q-dextran and ss-oligo, leading to a dissolution of the Q-dextran/ss-oligo phase. The internal PLL/ss-oligo phase also shrinks due to the enhanced macromolecular crowding and confinement.

Clearly, PEO exhibits more pronounced effect than dextran on regulating the phase separation of PLL, Q-dextran, and ss-oligo. It is mainly due to its nonspecific interactions with the internal phase. Interestingly, new morphologies are formed in their mixtures. For example, the coacervates grow into flower-like structures with Q-dextran/ss-oligo as the main body and PLL/ss-oligo as patches on the surface in 40.0 mg/mL PEO with 80.0 mg/mL dextran (Figure 5A). Such structure is not observed in any polymer solution containing single crowder, indicating that both PEO and dextran regulate the phase separation. To further demonstrate this point, we monitored the phase separation process in solution with the same PEO and dextran concentrations, but dextran was added afterward. The PLL/Q-dextran/ss-oligo droplets form network structures after 1 h in PEO solution (Figure 1D). Right after the addition of dextran, both the PLL/ss-oligo phase and the Q-dextran/ss-oligo phase in the network dissolve and shrink (Figure 5B and Movie S4). When only one lump is left in about 15 min, the fusion of the internal Q-dextran/ss-oligo subcompartments occurs, and the droplet turns into a shape different from flower-like structure, suggesting that LLPS in crowded medium is also controlled by kinetics.

The evolutional behavior of the droplets initially formed in dextran solution is more drastic as PEO is added afterward.

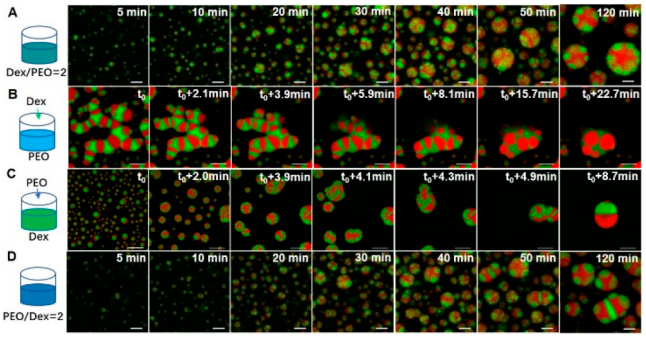

Figure 5. Coacervation of Q-dextran/PLL/ss-oligo in mixed PEO/Dextran media. (A) Flower-like structure formed in 40.0 mg/mL PEO with 80.0 mg/mL dextran. Scale bar: 5 μm. (B) Network of droplets formed in PEO solution evolve into a spherical droplet after the addition of dextran. The final concentrations of PEO and dextran are the same as that in (A). Scale bar: 10 μm. (C) Small size droplets formed in dextran grow and fuse into a giant Janus droplet after the addition of PEO. The final concentrations of PEO and dextran are 80.0 and 40.0 mg/mL, respectively. Scale bar: 50 μm. (D) Biphasic coacervates formed in mixed medium same as that in (C). Scale bar: 5 μm. The t_0 of (B) and (C) was 1 h.

PLL, Q-dextran, and ss-oligo form regular spherical biphasic droplets in dextran solution in 1 h (Figure 4D). The addition of PEO instantly causes a heavy merge of the particles. A gigantic droplet with mixed phases is formed in less than 10 min (Figure 5C and Movie S5). It eventually evolves into a Janus droplet with the diameter in the order of 0.1 mm, visible to naked eyes (Figure S4). The final concentrations of PEO and dextran are 80.0 and 40.0 mg/mL, respectively. If PEO and dextran are mixed beforehand, flower-like structures with less patches than that in Figure 5A are formed (Figure 5D). Semimerge of droplets caused by PLL/ss-oligo patches also occurs occasionally (Movie. S6).

In conclusion, the crowded medium generates profound effect on the LLPS processes. In general, the size of the phase(s) shrinks with increasing crowder concentration due to the macromolecular crowding and confinement effect. More importantly, a variety of morphologies are formed when the crowders have nonspecific interactions with the phase, especially the internal phase. Taken together, the LLPS could be controlled solely by the dynamic crowded environment. Since the crowded cellular interior contains a variety of background molecules, and each may possess certain affinity with the phase or subphases in the MLOs, the structure and functions of MLOs could be regulated by the crowed environment which is sensitive to the external variations.

■ ASSOCIATED CONTENT

Supporting Information

The Supporting Information is available free of charge at https://pubs.acs.org/doi/10.1021/acsmacrolett.2c00409.

Experimental section (PDF)
Formation of worm-like droplets at 6.0 mg/mL PEO (AVI)
Formation of coacervate network at 50.0 mg/mL PEO (AVI)
Phase inversion at 75.0 mg/mL PEO (AVI)
Phase transition in PEO/dextran mixture (AVI)
Giant Janus in dextran/PEO mixture (AVI)

https://doi.org/10.1021/acsmacrolett.2c00409
ACS Macro Lett. 2022, 11, 1107−1111

Connection of two droplets in PEO/dextran mixture (AVI)

AUTHOR INFORMATION

Corresponding Authors

Shuang Yang − *Beijing National Laboratory for Molecular Sciences, Department of Polymer Science and Engineering and the Key Laboratory of Polymer Chemistry and Physics of the Ministry of Education, College of Chemistry and Molecular Engineering, Peking University, Beijing 100871, China;* orcid.org/0000-0002-5573-5632; Email: shuangyang@pku.edu.cn

Dehai Liang − *Beijing National Laboratory for Molecular Sciences, Department of Polymer Science and Engineering and the Key Laboratory of Polymer Chemistry and Physics of the Ministry of Education, College of Chemistry and Molecular Engineering, Peking University, Beijing 100871, China;* orcid.org/0000-0003-4246-050X; Email: dliang@pku.edu.cn

Authors

Qingwen Bai − *Beijing National Laboratory for Molecular Sciences, Department of Polymer Science and Engineering and the Key Laboratory of Polymer Chemistry and Physics of the Ministry of Education, College of Chemistry and Molecular Engineering, Peking University, Beijing 100871, China*

Xu Chen − *Beijing National Laboratory for Molecular Sciences, Department of Polymer Science and Engineering and the Key Laboratory of Polymer Chemistry and Physics of the Ministry of Education, College of Chemistry and Molecular Engineering, Peking University, Beijing 100871, China*

Jiaxin Chen − *Beijing National Laboratory for Molecular Sciences, Department of Polymer Science and Engineering and the Key Laboratory of Polymer Chemistry and Physics of the Ministry of Education, College of Chemistry and Molecular Engineering, Peking University, Beijing 100871, China*

Zhijun Liu − *Beijing National Laboratory for Molecular Sciences, Department of Polymer Science and Engineering and the Key Laboratory of Polymer Chemistry and Physics of the Ministry of Education, College of Chemistry and Molecular Engineering, Peking University, Beijing 100871, China*

Ya-nan Lin − *Beijing National Laboratory for Molecular Sciences, Department of Polymer Science and Engineering and the Key Laboratory of Polymer Chemistry and Physics of the Ministry of Education, College of Chemistry and Molecular Engineering, Peking University, Beijing 100871, China*

Complete contact information is available at: https://pubs.acs.org/10.1021/acsmacrolett.2c00409

Author Contributions

‡Q.B. and X.C. contributed equally to this work.

Notes

The authors declare no competing financial interest.

ACKNOWLEDGMENTS

Financial support for this work from the National Natural Science Foundation of China (21774002 and 21973002) is gratefully acknowledged.

REFERENCES

(1) Mitrea, D. M.; Kriwacki, R. W. Phase separation in biology; functional organization of a higher order. *Cell Commun. Signal* **2016**, *14*, na.

(2) Decker, C. J.; Parker, R. P-bodies and stress granules: possible roles in the control of translation and mRNA degradation. *Cold Spring Harb Perspect Biol.* **2012**, *4* (9), a012286.

(3) Cho, W. K.; Spille, J. H.; Hecht, M.; Lee, C.; Li, C.; Grube, V.; Cisse, I. I. Mediator and RNA polymerase II clusters associate in transcription-dependent condensates. *Science* **2018**, *361* (6400), 412−415.

(4) Wu, X.; Cai, Q.; Feng, Z.; Zhang, M. Liquid-liquid phase separation in neuronal development and synaptic signaling. *Dev Cell* **2020**, *55*, 18−29.

(5) Woodruff, J. B.; Ferreira Gomes, B.; Widlund, P. O.; Mahamid, J.; Honigmann, A.; Hyman, A. A. The Centrosome is a selective condensate that nucleates microtubules by concentrating tubulin. *Cell* **2017**, *169* (6), 1066−1077.

(6) Feric, M.; Vaidya, N.; Harmon, T. S.; Mitrea, D. M.; Zhu, L.; Richardson, T. M.; Kriwacki, R. W.; Pappu, R. V.; Brangwynne, C. P. Coexisting liquid phases underlie nucleolar subcompartments. *Cell* **2016**, *165* (7), 1686−1697.

(7) Jain, S.; Wheeler, J. R.; Walters, R. W.; Agrawal, A.; Barsic, A.; Parker, R. ATPase-modulated stress granules contain a diverse proteome and substructure. *Cell* **2016**, *164* (3), 487−98.

(8) West, J. A.; Mito, M.; Kurosaka, S.; Takumi, T.; Tanegashima, C.; Chujo, T.; Yanaka, K.; Kingston, R. E.; Hirose, T.; Bond, C.; Fox, A.; Nakagawa, S. Structural, super-resolution microscopy analysis of paraspeckle nuclear body organization. *J. Cell Biol.* **2016**, *214* (7), 817−830.

(9) Simon, J. R.; Carroll, N. J.; Rubinstein, M.; Chilkoti, A.; Lopez, G. P. Programming molecular self-assembly of intrinsically disordered proteins containing sequences of low complexity. *Nat. Chem.* **2017**, *9* (6), 509−515.

(10) Zhao, H.; Ibrahimova, V.; Garanger, E.; Lecommandoux, S. Dynamic spatial formation and distribution of intrinsically disordered protein droplets in macromolecularly crowded protocells. *Angew. Chem. Int. Ed* **2020**, *59* (27), 11028−11036.

(11) Kaur, T.; Raju, M.; Alshareedah, I.; Davis, R. B.; Potoyan, D. A.; Banerjee, P. R. Sequence-encoded and composition-dependent protein-RNA interactions control multiphasic condensate morphologies. *Nat. Commun.* **2021**, *12* (1), na.

(12) Boeynaems, S.; Holehouse, A. S.; Weinhardt, V.; Kovacs, D.; Van Lindt, J.; Larabell, C.; Van Den Bosch, L.; Das, R.; Tompa, P. S.; Pappu, R. V.; Gitler, A. D. Spontaneous driving forces give rise to protein-RNA condensates with coexisting phases and complex material properties. *Proc. Natl. Acad. Sci.* **2019**, *116* (16), 7889−7898.

(13) Lu, T.; Spruijt, E. Multiphase Complex Coacervate Droplets. *J. Am. Chem. Soc.* **2020**, *142* (6), 2905−2914.

(14) Mountain, G. A.; Keating, C. D. Formation of multiphase complex coacervates and partitioning of biomolecules within them. *Biomacromolecules* **2020**, *21* (2), 630−640.

(15) Zimmerman, S. B.; Trach, S. O. Estimation of macromolecule concentrations and excluded volume effects for the cytoplasm of escherichia-coli. *J. Mol. Biol.* **1991**, *222* (3), 599−620.

(16) Rivas, G.; Minton, A. P. Macromolecular crowding in vitro, in vivo, and in between. *Trends Biochem. Sci.* **2016**, *41* (11), 970−981.

(17) Zhou, B.-R.; Liang, Y.; Du, F.; Zhou, Z.; Chen, J. Mixed macromolecular crowding accelerates the oxidative refolding of reduced, denatured lysozyme - Implications for protein folding in intracellular environments. *J. Biol. Chem.* **2004**, *279* (53), 55109−55116.

(18) van den Berg, B.; Ellis, R. J.; Dobson, C. M. Effects of macromolecular crowding on protein folding and aggregation. *EMBO J.* **1999**, *18* (24), 6927−6933.

(19) Li, J.; Zhang, S.; Wang, C. C. Effects of macromolecular crowding on the refolding of glucose-6-phosphate dehydrogenase and protein disulfide isomerase. *J. Biol. Chem.* **2001**, *276* (37), 34396−34401.

(20) Hatters, D. M.; Minton, A. P.; Howlett, G. J. Macromolecular crowding accelerates amyloid formation by human apolipoprotein C-II. *J. Biol. Chem.* **2002**, *277* (10), 7824−30.
(21) Akabayov, B.; Akabayov, S. R.; Lee, S.-J.; Wagner, G.; Richardson, C. C. Impact of macromolecular crowding on DNA replication. *Nat. Commun.* **2013**, *4* (1), na.
(22) Zimmerman, S. B.; Pheiffer, B. H. Macromolecular crowding allows blunt-end ligation by DNA ligases from rat liver or Escherichia coli. *Proc. Natl. Acad. Sci.* **1983**, *80* (19), 5852−6.
(23) Satyam, A.; Kumar, P.; Fan, X. L.; Gorelov, A.; Rochev, Y.; Joshi, L.; Peinado, H.; Lyden, D.; Thomas, B.; Rodriguez, B.; Raghunath, M.; Pandit, A.; Zeugolis, D. Macromolecular crowding meets tissue engineering by self-assembly: A paradigm shift in regenerative medicine. *Adv. Mater.* **2014**, *26* (19), 3024−3034.
(24) Ferreira, L. A.; Madeira, P. P.; Breydo, L.; Reichardt, C.; Uversky, V. N.; Zaslavsky, B. Y. Role of solvent properties of aqueous media in macromolecular crowding effects. *J. Biomol Struct Dyn* **2016**, *34* (1), 92−103.
(25) Breydo, L.; Sales, A. E.; Frege, T.; Howell, M. C.; Zaslavsky, B. Y.; Uversky, V. N. Effects of polymer hydrophobicity on protein structure and aggregation kinetics in crowded milieu. *Biochemistry* **2015**, *54* (19), 2957−66.
(26) King, J. T.; Arthur, E. J.; Brooks, C. L., 3rd; Kubarych, K. J. Crowding induced collective hydration of biological macromolecules over extended distances. *J. Am. Chem. Soc.* **2014**, *136* (1), 188−94.
(27) Verma, P. K.; Rakshit, S.; Mitra, R. K.; Pal, S. K. Role of hydration on the functionality of a proteolytic enzyme alpha-chymotrypsin under crowded environment. *Biochimie* **2011**, *93* (9), 1424−1433.
(28) Marianelli, A. M.; Miller, B. M.; Keating, C. D. Impact of macromolecular crowding on RNA/spermine complex coacervation and oligonucleotide compartmentalization. *Soft Matter* **2018**, *14* (3), 368−378.
(29) Wang, Y.; Latypov, R. F.; Lomakin, A.; Meyer, J. A.; Kerwin, B. A.; Vunnum, S.; Benedek, G. B. Quantitative evaluation of colloidal stability of antibody solutions using PEG-induced liquid−liquid phase separation. *Mol. Pharmaceutics* **2014**, *11* (5), 1391−1402.
(30) Julius, K.; Weine, J.; Gao, M.; Latarius, J.; Elbers, M.; Paulus, M.; Tolan, M.; Winter, R. Impact of macromolecular crowding and compression on protein−Protein Interactions and Liquid−Liquid Phase Separation Phenomena. *Macromolecules* **2019**, *52* (4), 1772−1784.
(31) Skóra, T.; Vaghefikia, F.; Fitter, J.; Kondrat, S. Macromolecular crowding: How shape and interactions affect diffusion. *J. Phys. Chem. B* **2020**, *124* (35), 7537−7543.
(32) Ferrolino, M. C.; Mitrea, D. M.; Michael, J. R.; Kriwacki, R. W. Compositional adaptability in NPM1-SURF6 scaffolding networks enabled by dynamic switching of phase separation mechanisms. *Nat. Commun.* **2018**, *9* (1), na.
(33) Park, S.; Barnes, R.; Lin, Y. X.; Jeon, Y. J.; Najafi, S.; Delaney, K. T.; Fredrickson, G. H.; Shea, J. E.; Hwang, D. S.; Han, S. Dehydration entropy drives liquid-liquid phase separation by molecular crowding. *Commun. Chem.* **2020**, *3* (1), na.
(34) Schuster, B. S.; Reed, E. H.; Parthasarathy, R.; Jahnke, C. N.; Caldwell, R. M.; Bermudez, J. G.; Ramage, H.; Good, M. C.; Hammer, D. A. Controllable protein phase separation and modular recruitment to form responsive membraneless organelles. *Nat. Commun.* **2018**, *9* (1), na.
(35) Ghosh, A.; Mazarakos, K.; Zhou, H.-X. Three archetypical classes of macromolecular regulators of protein liquid - liquid phase separation. *Proc. Nat. Acad. Sci.* **2019**, *116* (39), 19474−19483.
(36) André, A. A. M.; Spruijt, E. Liquid−Liquid Phase Separation in Crowded Environments. *Int. J. Mol. Sci.* **2020**, *21* (16), 5908.
(37) Bai, Q.; Zhang, Q.; Jing, H.; Chen, J.; Liang, D. Liquid−liquid phase separation of peptide/oligonucleotide complexes in crowded macromolecular media. *J. Phys. Chem. B* **2021**, *125* (1), 49−57.
(38) Jing, H. R.; Bai, Q. W.; Lin, Y. N.; Chang, H. J.; Yin, D. X.; Liang, D. H. Fission and internal fusion of protocell with membraneless "organelles" formed by liquid-liquid phase separation. *Langmuir* **2020**, *36* (27), 8017−8026.
(39) Chen, X.; Chen, E. Q.; Shi, A. C.; Yang, S. Multiphase coacervates driven by electrostatic correlations. *ACS Macro Lett.* **2021**, *10* (8), 1041−1047.
(40) Chao, S. H.; Schafer, J.; Gruebele, M. The surface of protein lambda(6−85) can act as a template for recurring Poly(ethylene glycol) structure. *Biochemistry* **2017**, *56* (42), 5671−5678.

https://doi.org/10.1021/acsmacrolett.2c00409
ACS Macro Lett. 2022, 11, 1107−1111